Isospin Amplitudes in $\Lambda_b^0 \to J/\psi \Lambda (\Sigma^0)$ and $\Xi_b^0 \to J/\psi \Xi^0 (\Lambda)$ Decays

R. Aaij *et al.*[*]

(LHCb Collaboration)

Ratios of isospin amplitudes in hadron decays are a useful probe of the interplay between weak and strong interactions and allow searches for physics beyond the standard model. We present the first results on isospin amplitudes in b-baryon decays, using data corresponding to an integrated luminosity of 8.5 fb^{-1}, collected with the LHCb detector in pp collisions at center of mass energies of 7, 8, and 13 TeV. The isospin amplitude ratio $|A_1(\Lambda_b^0 \to J/\psi \Sigma^0)/A_0(\Lambda_b^0 \to J/\psi \Lambda)|$, where the subscript on A indicates the final-state isospin, is measured to be less than $1/21.8$ at 95% confidence level. The Cabibbo suppressed $\Xi_b^0 \to J/\psi \Lambda$ decay is observed for the first time, allowing for the measurement $|A_0(\Xi_b^0 \to J/\psi \Lambda)/A_{1/2}(\Xi_b^0 \to J/\psi \Xi^0)| = 0.37 \pm 0.06 \pm 0.02$, where the uncertainties are statistical and systematic, respectively.

Measurements of ratios of isospin amplitudes A_i (i denotes the final-state isospin) in hadronic weak decays are a sensitive way to probe the interplay between strong and weak interactions. Such ratios can also reveal the presence of nonstandard model amplitudes. For example, in $K \to \pi\pi$ decays the experimentally determined ratio $|A_0/A_2| \approx 22.5$ has not been understood for over 50 years [1]. Recent models of the strong dynamics [2] and lattice gauge calculations [3] for these decays give only partial explanations. Determinations of isospin amplitudes from $D \to \pi\pi$ and $B \to \pi\pi$ decays, using input from other two-body decays into light hadrons, found $|A_0/A_2| \approx 2.5$ [4] and $|A_0/A_2| \approx 1.0$ [5], respectively.

In this Letter, we investigate $\Lambda_b^0 \to J/\psi \Lambda (\Sigma^0)$ and $\Xi_b^0 \to J/\psi \Xi^0 (\Lambda)$ decays. (Mention of a specific decay implies the use of its charge conjugate as well.) The leading order Feynman diagrams for all four processes are shown in Fig. 1. The isospins of the J/ψ meson and Λ baryon are zero, and that of the Σ^0 baryon is one. The isospin of the Λ_b^0 baryon is predicted by the quark model to be zero. Since the $b \to c\bar{c}s$ weak operator involves no isospin change, if this prediction is correct, we expect a dominant A_0 amplitude and a preference for the $J/\psi \Lambda$ final state over $J/\psi \Sigma^0$, which proceeds via the A_1 amplitude. Isospin breaking effects are possible due to the difference in mass and charge of the u and d quarks and can also be induced by QED, electroweak-penguin, or new physics processes [6]. If the Λ_b^0 baryon comprises a ud diquark, such effects should be small. Mixing of the Λ and Σ^0 baryons is also predicted to be small, $\sim 1°$, and could contribute ~ 0.01 to the $|A_1/A_0|$ amplitude ratio [7]. A severely suppressed $J/\psi \Sigma^0$ final state would determine the isospin of the Λ_b^0 baryon to be zero. Some previous LHCb analyses of Λ_b^0 decays made assumptions concerning isospin amplitudes. For instance, the pentaquark analysis, using the $\Lambda_b^0 \to J/\psi K^- p$ channel [8], assumed that the A_0 amplitude was dominant, and in the measurement of $|V_{ub}/V_{cb}|$ using $\Lambda_b^0 \to p\mu^-\bar{\nu}$ decays [9], the $A_{3/2}$ amplitude was assumed to be much smaller than the $A_{1/2}$ amplitude.

In $\Xi_b^0 \to J/\psi \Xi^0 (\Lambda)$ decays, taking the Ξ_b isospin as $1/2$, the final state results from an isospin change of zero ($1/2$) and has $A_i = A_{1/2}(A_0)$. In the reaction resulting in a final-state Λ baryon, the weak transition changes isospin due to the $b \to c\bar{c}d$ rather than the $b \to c\bar{c}s$ transition. Here we investigate if the larger isospin change is suppressed or if the decay amplitude is independent of the isospin change. Note that we measure the decay $\Xi_b^- \to J/\psi \Xi^-$ for two purposes: as a proxy for $\Xi_b^0 \to J/\psi \Xi^0$, which is difficult for us to measure, and to determine the background in $J/\psi \Lambda$ mass spectrum from these decays where $\Xi \to \Lambda\pi$.

The LHCb detector is a single-arm forward spectrometer covering the pseudorapidity range $2 < \eta < 5$, described in detail in Refs. [10,11]. The trigger [12] consists of a hardware stage, based on information from the calorimeter and muon systems, followed by a software stage, which reconstructs charged particles. Natural units are used here with $c = \hbar = 1$. We use data collected by the LHCb detector, corresponding to 1.0 fb^{-1} of integrated luminosity in 7 TeV pp collisions, 2.0 fb^{-1} at 8 TeV, and 5.5 fb^{-1} collected at 13 TeV. Hereafter, the data recorded at 7 and 8 TeV are referred to as run 1, and the data recorded at 13 TeV are referred to as run 2.
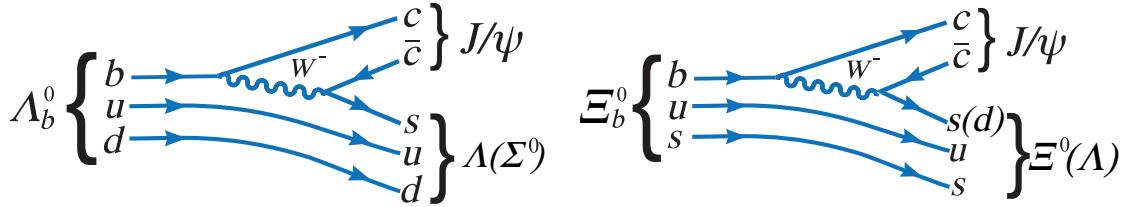
FIG. 1.   Leading order Feynman diagrams for $\Lambda_b^0 \to J/\psi\Lambda(\Sigma^0)$ and $\Xi_b^0 \to J/\psi\Xi^0(\Lambda)$ decays.

Simulation is required to model the effects of the detector acceptance and selection requirements. We generate pp collisions using PYTHIA [13] with a specific LHCb configuration [14]. Decays of unstable particles are described by EvtGen [15], where final-state radiation is generated using PHOTOS [16]. The interaction of the particles with the detector and its response are implemented using the GEANT4 toolkit [17] as described in Ref. [18]. The lifetimes for the Λ_b^0 and Ξ_b^- baryons are taken as 1.473 and 1.572 ps [19], respectively. All simulations are performed separately for runs 1 and 2.

Our strategy is to fully reconstruct the $J/\psi\Lambda$ final state and partially reconstruct the $J/\psi\Sigma^0$ mode by ignoring the photon from the $\Sigma^0 \to \gamma\Lambda$ decay, because of the low efficiency of the calorimeter at small photon energies. For these decays, the $J/\psi\Lambda$ mass distribution is almost uniform in the mass range 5350–5620 MeV. We simulate its shape and then fit the mass distribution to ascertain its size. The J/ψ meson is reconstructed through the $J/\psi \to \mu^+\mu^-$ decay. Candidates are formed by combining two oppositely charged tracks identified as muons, with transverse momentum $p_T > 550$ MeV. Each of the two muons are required to have a maximal χ^2 of distance of closest approach of 30 and are also required to form a vertex with $\chi^2_{\text{vtx}} < 16$. The J/ψ candidate is required to have a decay length significance from every primary vertex (PV) of greater than 3 and a mass in the range 3049–3140 MeV.

Candidate Λ baryons are formed from a pair of identified proton and π^- particles, each with momentum greater than 2 GeV. Because of their long lifetime and high boost, a majority of the Λ baryons decay after the vertex detector. However, we use only putative decays that occur inside the vertex detector. Each of the two tracks must be inconsistent with having originated from a PV, have a maximal χ^2 of distance of closest approach of 30, form a vertex with $\chi^2_{\text{vtx}} < 12$ that is separated from that PV by more than 3 standard deviations, and have a mass between 1105 and 1124 MeV. In addition, we eliminate candidates that when interpreted as $\pi^+\pi^-$ fall within 7.5 MeV of the known K_S^0 mass. Candidate $\Xi^- \to \Lambda\pi^-$ decays are reconstructed using the criteria in Ref. [20], with the additional requirement that the Ξ^- decays in the LHCb vertex detector. These are combined with selected J/ψ mesons to form candidate Ξ_b^- baryons.

We improve the $J/\psi\Lambda$ mass resolution by constraining the J/ψ and Λ candidates to their known masses and their decay products to originate from each of the relevant decay

vertices; we also constrain the J/ψ and the Λ candidates to come from the same decay point [21].

After these selections, we use two boosted decision trees (BDTs) [22,23] implemented in the TMVA toolkit [24] to further separate signal from background. The first BDT is trained to reject generic $b \to J/\psi X$ decays, where X contains one or more charged tracks. We train this "isolation" BDT using the following information: the χ^2_{IP} of additional charged tracks with respect to the J/ψ vertex, where χ^2_{IP} is defined as the difference in the χ^2_{vtx} of the J/ψ vertex reconstructed with and without the track being considered, the χ^2_{vtx} of the vertex formed by the J/ψ plus each additional track, the minimum χ^2_{IP} of the additional track with respect to any PV, and the p_T of the additional track. For the isolation BDT training, we use samples of $\Lambda_b^0 \to J/\psi\Lambda$ and $B^- \to J/\psi K^-$ candidates for the signal and background models, respectively. Both samples are background subtracted using the "sPlot" technique [25]. The output of the isolation BDT is used as an input variable in the final BDT.

The 20 discrimination variables used in the final BDT are listed in the Supplemental Material [26]. These mostly exploit the topology of the decay using the vertexing properties of the J/ψ, Λ, and Λ_b^0 candidates and particle identification of their decay products. The signal sample again is background subtracted $\Lambda_b^0 \to J/\psi\Lambda$ combinations. For background training, we use candidates in the upper sideband with $J/\psi\Lambda$ masses between 5.7 and 6.0 GeV, excluding events in 5.77–5.81 GeV to avoid including $\Xi_b^0 \to J/\psi\Lambda$ decays in the background sample. We use k-folding cross validation with five folds in both BDTs to avoid any possible bias [27]. The final BDT selection is optimized to maximize the Punzi figure of merit, $\epsilon_s/(\sqrt{B} + 1.5)$ [28], where ϵ_s is the efficiency of the final BDT selection on simulated $\Lambda_b^0 \to J/\psi\Sigma^0$ decays and B is the number of background candidates in the above defined sideband that pass the BDT requirement, scaled to the width of the $J/\psi\Sigma^0$ signal window. The analysis is performed separately on run 1 and run 2 data. The resulting $J/\psi\Lambda$ mass spectrum for run 2 data is shown in Fig. 2. The run 1 mass distribution is similar and is shown in the Supplemental Material [26].

There are two signal peaks evident in the mass distribution in Fig. 2. The larger is due to $\Lambda_b^0 \to J/\psi\Lambda$ decays, and the smaller corresponds to $\Xi_b^0 \to J/\psi\Lambda$ decays. The
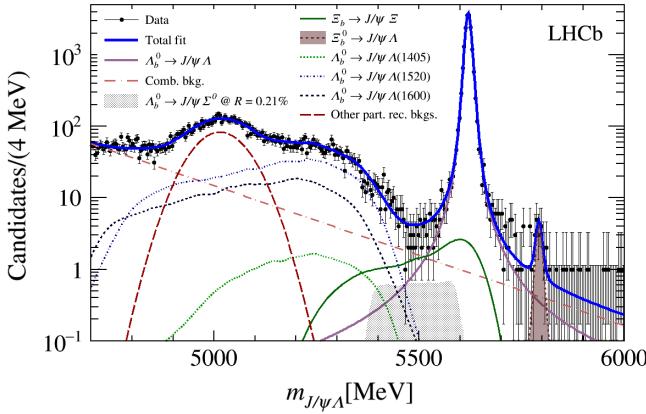
FIG. 2. Distribution of the $J/\psi\Lambda$ mass for run 2 data. Error bars without data points indicate empty bins. Also shown is the projection of the joint fit to the data. The thick (blue) solid curve shows the total fit. For illustrative purposes, the $\Lambda_b^0 \to J/\psi\Sigma^0$ signal component is artificially scaled to its measured upper limit. The shapes are identified in the legend.

latter is a heretofore unobserved Cabibbo suppressed decay. The run 1 and 2 mass distribution data are fit jointly to determine the $\Lambda_b^0 \to J/\psi\Lambda$, $\Lambda_b^0 \to J/\psi\Sigma^0$, and $\Xi_b^0 \to J/\psi\Lambda$ yields. The $\Lambda_b^0 \to J/\psi\Sigma^0$ signal is modeled using a Gaussian kernel [29] shape fit to simulation. The $\Lambda_b^0 \to J/\psi\Lambda$ signal is described by a Hypatia function, whose tail parameters are fixed from simulation, with the mass and width allowed to vary in the fit to the data [30]. The $\Xi_b^0 \to J/\psi\Lambda$ peak is fit to the same shape but with its mean constrained to the fitted Λ_b^0 mass plus the known $\Xi_b^0 - \Lambda_b^0$ mass difference of 172.5 MeV [19].

While most of the candidates above the Λ_b^0 peak are the result of combinatoric background, those below are due to additional sources. One is due to $\Lambda_b^0 \to J/\psi\Lambda^*$ decays, with $\Lambda^* \to \Sigma^0\pi^0$ and $\Sigma^0 \to \gamma\Lambda$. Here, Λ^* denotes strange baryon resonances ranging from 1405 to 2350 MeV in mass. Another source comprises partially reconstructed $\Lambda_b^0 \to \psi(2S)\Lambda$ decays, where $\psi(2S) \to \pi\pi J/\psi$. These decays mainly populate masses lower than the $\Lambda_b^0 \to J/\psi\Sigma^0$ signal, but need to be included to accurately model the combinatoric background. The existence of the $\Lambda_b^0 \to J/\psi\Lambda^*$ channels was demonstrated in a study of $\Lambda_b^0 \to J/\psi K^- p$ decays [8]. We can model the resulting $J/\psi\Lambda$ mass shapes of the different $\Lambda_b^0 \to J/\psi\Lambda^*$ backgrounds, although we do not know their yields due to lack of knowledge of the relative $\Lambda^* \to \Sigma^0\pi^0$ branching fractions. We use separate shapes in the fit for the backgrounds corresponding to the $\Lambda(1405)$, $\Lambda(1520)$, and $\Lambda(1600)$ resonances. These backgrounds are simulated, processed through the event selections, and fit using Gaussian kernel shapes. We collectively model the sum of the remaining Λ^* and $\psi(2S)$ backgrounds in the fit using a Gaussian shape. Note that our aim here is not to accurately disentangle each

source of background, but only to model their collective sum.

A third background source arises from $\Xi_b \to J/\psi\Xi$ decays, where $\Xi \to \Lambda\pi$, when the pion from the Ξ decay is not reconstructed. This background is modeled by a Gaussian kernel shape fit to simulated $\Xi_b^- \to J/\psi\Xi^-$ decays, which are partially reconstructed as $J/\psi\Lambda$. The normalization of this background is determined by fully reconstructing $\Xi_b^- \to J/\psi\Xi^-$ decays in data and simulation to obtain an efficiency-corrected yield. The reconstruction uses the criteria in Ref. [20]. The reconstructed $J/\psi\Xi^-$ mass distribution in data is shown in the Supplemental Material [26]. The efficiency-corrected yield is multiplied by the relative efficiency of reconstructing $\Xi_b^- \to J/\psi\Xi^-$, as $J/\psi\Lambda$, and then more than doubled to account for $\Xi_b^0 \to J/\psi\Xi^0$ decays. The production rates are unequal mostly because the $\Xi_b'(5935)^0$ state is too light to decay into $\Xi_b^-\pi^+$, so it always decays into Ξ_b^0 [31]. In addition, we incorporate the production measurements of other excited Ξ_b resonances [32] to determine the inclusive production ratio of $\Xi_b^0/\Xi_b^- = 1.37 \pm 0.07$, where the uncertainty arises mainly from the production fraction measurements of the excited states. We further corrected for the lifetime ratio $\tau_{\Xi_b^-}/\tau_{\Xi_b^0} = 1.08 \pm 0.04$ [33]. This normalization is introduced into the final fit as a Gaussian constraint and done separately for run 1 and run 2 data, as the detection efficiencies differ.

The remaining background comes mostly from random combinations of real J/ψ and Λ, which contribute both above and below the $\Lambda_b^0 \to J/\psi\Lambda$ mass peak. This combinatoric background is modeled using an exponential function.

The run 1 and run 2 mass distribution data are fit simultaneously, using a binned extended maximum-likelihood fit, where the efficiency-corrected relative yields of the $\Lambda_b^0 \to J/\psi\Sigma^0$ signal, and those of the three $\Lambda_b^0 \to J/\psi\Lambda^*$ decays, with respect to the $\Lambda_b^0 \to J/\psi\Lambda$ signal, are constrained to be the same in the two datasets. We define

$$\mathcal{R} \equiv \frac{|A_1|^2}{|A_0|^2} = \frac{\mathcal{B}(\Lambda_b^0 \to J/\psi\Sigma^0)}{\mathcal{B}(\Lambda_b^0 \to J/\psi\Lambda)}\Phi_{\Lambda_b^0}$$

$$= \frac{N_{\Lambda_b^0 \to J/\psi\Sigma}}{N_{\Lambda_b^0 \to J/\psi\Lambda}}\frac{\epsilon_{\Lambda_b^0 \to J/\psi\Lambda}}{\epsilon_{\Lambda_b^0 \to J/\psi\Sigma}}\Phi_{\Lambda_b^0}, \quad (1)$$

where $N_{\Lambda_b^0 \to J/\psi\Sigma}$ and $N_{\Lambda_b^0 \to J/\psi\Lambda}$ are the yields of the $\Lambda_b^0 \to J/\psi\Sigma$ and $\Lambda_b^0 \to J/\psi\Lambda$ decays, and $\epsilon_{\Lambda_b^0 \to J/\psi\Sigma}$ and $\epsilon_{\Lambda_b^0 \to J/\psi\Lambda}$ are their respective efficiencies, as estimated from simulation. The phase space correction factor $\Phi_{\Lambda_b^0}$ is 1.058. The free parameters of interest in the fit are $\mathcal{R}$, $N_{\Lambda_b^0 \to J/\psi\Lambda}$, and $N_{\Xi_b^0 \to J/\psi\Lambda}$; $N_{\Lambda_b^0 \to J/\psi\Sigma}$ can be calculated from these. Systematic uncertainties are folded into the fit components as Gaussian constraints. These include uncertainties on the simulated ratios of efficiencies for the different Λ_b^0 final

states with respect to the $J/\psi\Lambda$ final state, which range from 1.4% to 2.4%. The uncertainty of the relative normalization of the $\Xi_b \to J/\psi\Xi$ background is estimated to be 12.1% for run 1 and 9.8% for run 2. This has contributions from the fit yield of the fully reconstructed $\Xi_b^- \to J/\psi\Xi^-$ decay, the reconstruction and efficiency of finding the $\Xi^- \to \Lambda\pi^-$ decay, and the Ξ_b^-/Ξ_b^0 lifetime ratio.

The results of the fit are shown in Fig. 2 and reported in Table I. The fitted value for $\mathcal{R}$ is consistent with zero. In Fig. 2, we illustrate what this component would look like if observed at the upper limit on $\mathcal{R}$. We do not quote the yields of the $\Lambda_b^0 \to J/\psi\Lambda^*$ decays, as these are highly correlated.

To set an upper limit on $\mathcal{R}$, we use the *CLs* method [34]. The variation of the observed and expected *CLs* versus $\mathcal{R}$ is scanned from 0 to 0.005 and shown in Fig. 3. Our observed upper limit on $\mathcal{R}$ is

$$\mathcal{R} < 0.0021 \quad \text{at } 95\% \text{ C.L.}$$

Systematic uncertainties are incorporated in the fit and included in this limit. Further consistency checks include changing the fit range, eliminating the $\Lambda_b^0 \to J/\psi\Lambda^*$ background components one at a time, and fitting the $\Lambda_b^0 \to J/\psi\Lambda$ peak with different functions. These change the upper limit only by small amounts.

The run 1 and run 2 signal yields for $\Xi_b^0 \to J/\psi\Lambda$ are listed in Table I. The statistical significance of the $\Xi_b^0 \to J/\psi\Lambda$ signal is 5.6 standard deviations, obtained using Wilks's theorem [35], and includes both the statistical and systematic uncertainties. The branching fraction ratio $\mathcal{B}(\Xi_b^0 \to J/\psi\Lambda)/\mathcal{B}(\Xi_b^0 \to J/\psi\Xi^0)$ is determined using the fully reconstructed $\Xi_b^- \to J/\psi\Xi^-$ sample described above. To determine the branching fraction of $\mathcal{B}(\Xi_b^0 \to J/\psi\Xi^0)$, we assume equal decay widths for the two different $\Xi_b \to J/\psi\Xi$ charge states and correct for the different neutral and charged Ξ_b production rates as described above. We use the measured lifetime ratio [33] to translate the decay width equality into the needed branching fraction. The run 1 and run 2 results are consistent. Combining the two, we find

$$R_{\Xi_b} \equiv \frac{\mathcal{B}(\Xi_b^0 \to J/\psi\Lambda)}{\mathcal{B}(\Xi_b^0 \to J/\psi\Xi^0)} = (8.2 \pm 2.1 \pm 0.9) \times 10^{-3},$$

TABLE I. Results from the fit to the $J/\psi\Lambda$ mass distribution. The fitted yields are indicated by N. Note $N_{\Xi_b \to J/\psi\Xi}$ indicates the sum of Ξ_b^- and Ξ_b^0 decays.

Parameter	Shared value	Run 1 value	Run 2 value
$\mathcal{R}$	$(0 \pm 5.3) \times 10^{-4}$	$\cdots$	$\cdots$
$N_{\Lambda_b^0 \to J/\psi\Lambda}$	$\cdots$	4417 ± 66	16970 ± 130
$N_{\Xi_b \to J/\psi\Xi}$	$\cdots$	23.3 ± 5.7	139.7 ± 21.9
$N_{\Xi_b^0 \to J/\psi\Lambda}$	$\cdots$	6.2 ± 3.0	17.8 ± 5.1

where the first uncertainty is statistical the second is systematic, where the leading source is the systematic uncertainty in the $\Xi_b^- \to J/\psi\Xi^-$ fit yield.

We convert R_{Ξ_b} into a measurement of the amplitude ratio

$$\left|\frac{A_0}{A_{1/2}}\right| = \frac{1}{\lambda}\sqrt{\frac{R_{\Xi_b}}{\Phi_{\Xi_b}}} = 0.37 \pm 0.06 \pm 0.02,$$

where $\Phi_{\Xi_b} = 1.15$ is the relative phase space factor, and $\lambda = 0.231$ is the relative Cabibbo suppression $|V_{cd}|/|V_{cs}|$, which is assumed equal to $|V_{us}|/|V_{ud}|$ [19]. Taking the s and u quarks in the Ξ_b^0 baryon to be a diquark state with isospin $1/2$ and combining with the null isospin of the s quark from the b quark decay leads to isospin $1/2$ for the $J/\psi\Xi^0$ final state. On the other hand, for the Cabibbo suppressed transition with the isospin $1/2$ d quark, we have either isospin 0 or 1 final states. The former corresponds to $J/\psi\Lambda$, with the latter to $J/\psi\Sigma^0$, which we cannot currently measure. In order to predict the expected ratio of isospin amplitudes the SU(3) flavor [36] b-baryon couplings must be taken into account [37]. Then, if there are no other amplitudes, the theoretically predicted ratio corresponding to no preference between isospin 0 and $1/2$ amplitudes is $|A_0/A_{1/2}|$ equal to $1/\sqrt{6}$ (≈ 0.41). Therefore, our result is consistent with no suppression of the isospin changing amplitude. These results are not precise enough to see the effects of SU(3) flavor symmetry breaking.

In conclusion, we set an upper limit in $\Lambda_b^0 \to J/\psi\Lambda(\Sigma^0)$ decays on the isospin amplitude ratio

$$|A_1/A_0| = \sqrt{\mathcal{R}} < 1/21.8 \quad \text{at } 95\% \text{ C.L.}$$
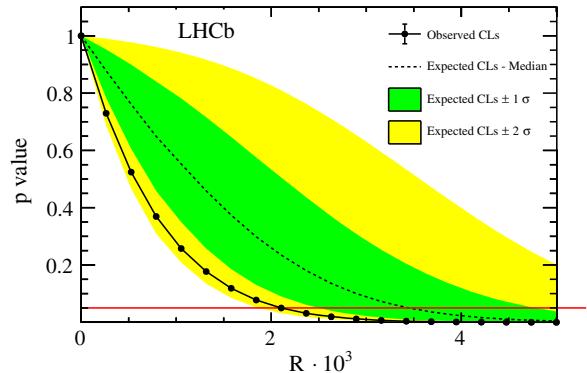
FIG. 3. Result of the hypothesis tests conducted using the *CLs* method by varying $\mathcal{R}$ is shown. The observed *CLs* distribution is shown by the round (black) points. The expected *CLs* distribution (based on the background only hypothesis) is shown by the dashed line (black), with 1 and 2σ uncertainty bands depicted in dark shaded (green) and light shaded (yellow) bands. The observed and expected upper limits are obtained by seeing where the bands cross the p value of 0.05 shown as the horizontal (red) line.

This limit is stringent and rules out isospin violation at an $\sim 1\%$ rate. Isospin violation has been seen at this level, for example, in $\rho - \omega$ mixing in $\bar{B}^0 \to J/\psi \pi^+ \pi^-$ decays [38]. Our limit is consistent with the Λ_b^0 being formed of a b quark and a ud diquark. This measurement also constrains nonstandard model A_1 amplitudes contributing to Λ_b^0 decays. Furthermore, our results support the quark model prediction of the Λ_b^0 being an isosinglet. Assumptions of isospin suppression in $\Lambda_b^0 \to J/\psi X$ decays made in past analyses are shown to be justified. Finally, we report the discovery of the Cabibbo suppressed decay $\Xi_b^0 \to J/\psi \Lambda$ and measure its branching fraction relative to $\Xi_b^0 \to J/\psi \Xi^0$ to be $(8.2 \pm 2.1 \pm 0.9) \times 10^{-3}$. We see no evidence for the preference of either isospin amplitude in the ratio $|A_0/A_{1/2}| = 0.37 \pm 0.06 \pm 0.02 \pm 0.1$, as the prediction for the equality of isospin amplitudes is $1/\sqrt{6}$.

[1] H.-Y. Cheng, Status of the $\Delta I = 1/2$ rule in kaon decay, Int. J. Mod. Phys. A **04**, 495 (1989).

[2] A. J. Buras, J.-M. Gérard, and W. A. Bardeen, Large N approach to kaon decays and mixing 28 years later: $\Delta I = 1/2$ rule, $\hat{B}_K$ and ΔM_K, Eur. Phys. J. C **74**, 2871 (2014).

[3] P. A. Boyle *et al.* (RBC and UKQCD Collaborations), Emerging Understanding of the $\Delta I = 1/2$ Rule from Lattice QCD, Phys. Rev. Lett. **110**, 152001 (2013); T. Blum *et al.*, $K \to \pi\pi \Delta I = 3/2$ decay amplitude in the continuum limit, Phys. Rev. D **91**, 074502 (2015); N. Ishizuka, K.-I. Ishikawa, A. Ukawa, and T. Yoshié, Calculation of $K \to \pi\pi$ decay amplitudes with improved Wilson fermion action in lattice QCD, Phys. Rev. D **92**, 074503 (2015).

[4] E. Franco, S. Mishima, and L. Silvestrini, The standard model confronts CP violation in $D^0 \to \pi^+\pi^-$ and $D^0 \to K^+K^-$, J. High Energy Phys. 05 (2012) 140.

[5] B. Grinstein, D. Pirtskhalava, D. Stone, and P. Uttayarat, B decays to two pseudoscalars and a generalized $\Delta I = \frac{1}{2}$ rule, Phys. Rev. D **89**, 114014 (2014).

[6] Y. Grossman, M. Neubert, and A. L. Kagan, Trojan penguins and isospin violation in hadronic B decays, J. High Energy Phys. 10 (1999) 029.

[7] S. R. Coleman and S. L. Glashow, Electrodynamic Properties of Baryons in the Unitary Symmetry Scheme, Phys. Rev. Lett. **6**, 423 (1961); R. H. Dalitz and F. Von Hippel, Electromagnetic $\Lambda - \Sigma^0$ mixing and charge symmetry for the Λ-hyperon, Phys. Lett. **10**, 153 (1964); Z. R. Kordov, R. Horsley, Y. Nakamura, H. Perlt, P. E. L. Rakow, G. Schierholz, H. Stüben, R. D. Young, and J. M. Zanotti (CSSM/QCDSF/UKQCD Collaborations), Electromagnetic contribution to Σ-Λ mixing using lattice QCD + QED, Phys. Rev. D **101**, 034517 (2020).

[8] R. Aaij *et al.* (LHCb Collaboration), Observation of $J/\psi p$ Resonances Consistent with Pentaquark States in $\Lambda_b^0 \to J/\psi K^- p$ Decays, Phys. Rev. Lett. **115**, 072001 (2015).

[9] R. Aaij *et al.* (LHCb Collaboration), Determination of the quark coupling strength $|V_{ub}|$ using baryonic decays, Nat. Phys. **11**, 743 (2015).

[10] A. A. Alves, Jr. *et al.* (LHCb Collaboration), The LHCb detector at the LHC, J. Instrum. **3**, S08005 (2008).

[11] R. Aaij *et al.* (LHCb Collaboration), LHCb detector performance, Int. J. Mod. Phys. A **30**, 1530022 (2015).

[12] R. Aaij *et al.*, The LHCb trigger and its performance in 2011, J. Instrum. **8**, P04022 (2013).

[13] T. Sjöstrand, S. Mrenna, and P. Skands, A brief introduction to PYTHIA 8.1, Comput. Phys. Commun. **178** (2008) 852; PYTHIA 6.4 physics and manual, J. High Energy Phys. 05 (2006) 026.

[14] I. Belyaev *et al.*, Handling of the generation of primary events in Gauss, the LHCb simulation framework, J. Phys. Conf. Ser. **331**, 032047 (2011).

[15] D. J. Lange, The EvtGen particle decay simulation package, Nucl. Instrum. Methods Phys. Res., Sect. A **462**, 152 (2001).

[16] P. Golonka and Z. Was, PHOTOS Monte Carlo: A precision tool for QED corrections in Z and W decays, Eur. Phys. J. C **45**, 97 (2006).

[17] J. Allison *et al.* (GEANT4 Collaboration), Geant4 developments and applications, IEEE Trans. Nucl. Sci. **53** (2006) 270; S. Agostinelli *et al.* (GEANT4 Collaboration), GEANT4: A simulation toolkit, Nucl. Instrum. Methods Phys. Res., Sect. A **506**, 250 (2003).

[18] M. Clemencic, G. Corti, S. Easo, C. R. Jones, S. Miglioranzi, M. Pappagallo, and P. Robbe, The LHCb simulation

application, Gauss: Design, evolution and experience, J. Phys. Conf. Ser. **331**, 032023 (2011).

[19] M. Tanabashi *et al.* (Particle Data Group), Review of particle physics, Phys. Rev. D **98**, 030001 (2018), and 2019 update.

[20] R. Aaij *et al.* (LHCb Collaboration), Measurement of the mass and production rate of Ξ_b^- baryons, Phys. Rev. D **99**, 052006 (2019).

[21] W. D. Hulsbergen, Decay chain fitting with a Kalman filter, Nucl. Instrum. Methods Phys. Res., Sect. A **552**, 566 (2005).

[22] L. Breiman, J. H. Friedman, R. A. Olshen, and C. J. Stone, *Classification and Regression Trees* (Wadsworth International Group, Belmont, CA, 1984).

[23] R. E. Schapire and Y. Freund, A decision-theoretic generalization of on-line learning and an application to boosting, J. Comput. Syst. Sci. **55**, 119 (1997).

[24] A. Hoecker *et al.*, TMVA: Toolkit for multivariate data analysis, Proc. Sci. ACAT2007 (**2007**) 040 [arXiv:physics/0703039]; J. Stelzer, A. Hocker, P. Speckmayer, and H. Voss, Current developments in TMVA: An outlook to TMVA4, Proc. Sci. ACAT08 (**2008**) 063.

[25] M. Pivk and F. R. Le Diberder, sPlot: A Statistical tool to unfold data distributions, Nucl. Instrum. Methods Phys. Res., Sect. A **555**, 356 (2005).

[26] See Supplemental Material at http://link.aps.org/supplemental/10.1103/PhysRevLett.124.111802 for main BDT input variables in Sect. A.1, the projection of the fit to the Run 1 $J/\psi\Lambda$ mass spectrum in Sect. A.2, and the fits to the $J/\psi\Xi^-$ mass spectra in Sect. A.3.

[27] A. Bagoly, A. Bevan, A. Carnes, S. V. Gleyzer, L. Moneta, A. Moudgil, S. Pfreundschuh, T. Stevenson, S. Wunsch,

and O. Zapata, Machine learning developments in ROOT, J. Phys. Conf. Ser. **898**, 072046 (2017).

[28] G. Punzi, Sensitivity of searches for new signals and its optimization, eConf **C030908**, MODT002 (2003).

[29] K. S. Cranmer, Kernel estimation in high-energy physics, Comput. Phys. Commun. **136**, 198 (2001).

[30] D. Martinez Santos and F. Dupertuis, Mass distributions marginalized over per-event errors, Nucl. Instrum. Methods Phys. Res., Sect. A **764**, 150 (2014).

[31] R. Aaij *et al.* (LHCb Collaboration), Observation of Two New Ξ_b^- Baryon Resonances, Phys. Rev. Lett. **114**, 062004 (2015).

[32] R. Aaij *et al.* (LHCb Collaboration), Measurement of the properties of the Ξ_b^{*0} baryon, J. High Energy Phys. 05 (2016) 161.

[33] R. Aaij *et al.* (LHCb Collaboration), Precision Measurement of the Mass and Lifetime of the Ξ_b^- Baryon, Phys. Rev. Lett. **113**, 242002 (2014).

[34] A. L. Read, Presentation of search results: The CL_s technique, J. Phys. G **28**, 2693 (2002).

[35] S. S. Wilks, The large-sample distribution of the likelihood ratio for testing composite hypotheses, Ann. Math. Stat. **9**, 60 (1938).

[36] G. Hiller, M. Jung, and S. Schacht, $SU(3)_F$ in nonleptonic charm decays, Proc. Sci. EPS-HEP2013 (**2013**) 371.

[37] A. Dery, M. Ghosh, Y. Grossman, and S. Schacht, $SU(3)_F$ analysis for beauty baryon decays, arXiv:2001.05397.

[38] R. Aaij *et al.* (LHCb Collaboration), Measurement of the CP-violating phase β in $\bar{B}^0 \to J/\psi\pi^+\pi^-$ decays and limits on penguin effects, Phys. Lett. B **742**, 38 (2015).

R. Aaij,[31] C. Abellán Beteta,[49] T. Ackernley,[59] B. Adeva,[45] M. Adinolfi,[53] H. Afsharnia,[9] C. A. Aidala,[80] S. Aiola,[25] Z. Ajaltouni,[9] S. Akar,[66] P. Albicocco,[22] J. Albrecht,[14] F. Alessio,[47] M. Alexander,[58] A. Alfonso Albero,[44] G. Alkhazov,[37] P. Alvarez Cartelle,[60] A. A. Alves Jr.,[45] S. Amato,[2] Y. Amhis,[11] L. An,[21] L. Anderlini,[21] G. Andreassi,[48] M. Andreotti,[20] F. Archilli,[16] J. Arnau Romeu,[10] A. Artamonov,[43] M. Artuso,[67] K. Arzymatov,[41] E. Aslanides,[10] M. Atzeni,[49] B. Audurier,[26] S. Bachmann,[16] J. J. Back,[55] S. Baker,[60] V. Balagura,[11,a] W. Baldini,[20,47] A. Baranov,[41] R. J. Barlow,[61] S. Barsuk,[11] W. Barter,[60] M. Bartolini,[23,47,b] F. Baryshnikov,[77] G. Bassi,[28] V. Batozskaya,[35] B. Batsukh,[67] A. Battig,[14] A. Bay,[48] M. Becker,[14] F. Bedeschi,[28] I. Bediaga,[1] A. Beiter,[67] L. J. Bel,[31] V. Belavin,[41] S. Belin,[26] N. Beliy,[5] V. Bellee,[48] K. Belous,[43] I. Belyaev,[38] G. Bencivenni,[22] E. Ben-Haim,[12] S. Benson,[31] S. Beranek,[13] A. Berezhnoy,[39] R. Bernet,[49] D. Berninghoff,[16] H. C. Bernstein,[67] C. Bertella,[47] E. Bertholet,[12] A. Bertolin,[27] C. Betancourt,[49] F. Betti,[19,c] M. O. Bettler,[54] Ia. Bezshyiko,[49] S. Bhasin,[53] J. Bhom,[33] M. S. Bieker,[14] S. Bifani,[52] P. Billoir,[12] A. Bizzeti,[21,d] M. Bjørn,[62] M. P. Blago,[47] T. Blake,[55] F. Blanc,[48] S. Blusk,[67] D. Bobulska,[58] V. Bocci,[30] O. Boente Garcia,[45] T. Boettcher,[63] A. Boldyrev,[78] A. Bondar,[42,e] N. Bondar,[37] S. Borghi,[61,47] M. Borisyak,[41] M. Borsato,[16] J. T. Borsuk,[33] T. J. V. Bowcock,[59] C. Bozzi,[20] M. J. Bradley,[60] S. Braun,[16] A. Brea Rodriguez,[45] M. Brodski,[47] J. Brodzicka,[33] A. Brossa Gonzalo,[55] D. Brundu,[26] E. Buchanan,[53] A. Buonaura,[49] C. Burr,[47] A. Bursche,[26] J. S. Butter,[31] J. Buytaert,[47] W. Byczynski,[47] S. Cadeddu,[26] H. Cai,[72] R. Calabrese,[20,f] L. Calero Diaz,[22] S. Cali,[22] R. Calladine,[52] M. Calvi,[24,g] M. Calvo Gomez,[44,h] P. Camargo Magalhaes,[53] A. Camboni,[44,h] P. Campana,[22] D. H. Campora Perez,[31] L. Capriotti,[19,c] A. Carbone,[19,c] G. Carboni,[29] R. Cardinale,[23,b] A. Cardini,[26] P. Carniti,[24,g] K. Carvalho Akiba,[31] A. Casais Vidal,[45] G. Casse,[59] M. Cattaneo,[47] G. Cavallero,[47] S. Celani,[48] R. Cenci,[28,i] J. Cerasoli,[10] M. G. Chapman,[53] M. Charles,[12,47] Ph. Charpentier,[47] G. Chatzikonstantinidis,[52] M. Chefdeville,[8] V. Chekalina,[41] C. Chen,[3] S. Chen,[26] A. Chernov,[33] S.-G. Chitic,[47] V. Chobanova,[45] M. Chrzaszcz,[33] A. Chubykin,[37] P. Ciambrone,[22] M. F. Cicala,[55] X. Cid Vidal,[45] G. Ciezarek,[47] F. Cindolo,[19] P. E. L. Clarke,[57] M. Clemencic,[47] H. V. Cliff,[54]

J. Closier,[47] J. L. Cobbledick,[61] V. Coco,[47] J. A. B. Coelho,[11] J. Cogan,[10] E. Cogneras,[9] L. Cojocariu,[36] P. Collins,[47] T. Colombo,[47] A. Comerma-Montells,[16] A. Contu,[26] N. Cooke,[52] G. Coombs,[58] S. Coquereau,[44] G. Corti,[47] C. M. Costa Sobral,[55] B. Couturier,[47] D. C. Craik,[63] J. Crkovská,[66] A. Crocombe,[55] M. Cruz Torres,[1,j] R. Currie,[57] C. L. Da Silva,[66] E. Dall'Occo,[14] J. Dalseno,[45,53] C. D'Ambrosio,[47] A. Danilina,[38] P. d'Argent,[16] A. Davis,[61] O. De Aguiar Francisco,[47] K. De Bruyn,[47] S. De Capua,[61] M. De Cian,[48] J. M. De Miranda,[1] L. De Paula,[2] M. De Serio,[18,k] P. De Simone,[22] J. A. de Vries,[31] C. T. Dean,[66] W. Dean,[80] D. Decamp,[8] L. Del Buono,[12] B. Delaney,[54] H.-P. Dembinski,[15] M. Demmer,[14] A. Dendek,[34] V. Denysenko,[49] D. Derkach,[78] O. Deschamps,[9] F. Desse,[11] F. Dettori,[26] B. Dey,[7] A. Di Canto,[47] P. Di Nezza,[22] S. Didenko,[77] H. Dijkstra,[47] V. Dobishuk,[51] F. Dordei,[26] M. Dorigo,[28,l] A. C. dos Reis,[1] L. Douglas,[58] A. Dovbnya,[50] K. Dreimanis,[59] M. W. Dudek,[33] L. Dufour,[47] G. Dujany,[12] P. Durante,[47] J. M. Durham,[66] D. Dutta,[61] M. Dziewiecki,[16] A. Dziurda,[33] A. Dzyuba,[37] S. Easo,[56] U. Egede,[69] V. Egorychev,[38] S. Eidelman,[42,e] S. Eisenhardt,[57] R. Ekelhof,[14] S. Ek-In,[48] L. Eklund,[58] S. Ely,[67] A. Ene,[36] E. Epple,[66] S. Escher,[13] S. Esen,[31] T. Evans,[47] A. Falabella,[19] J. Fan,[3] N. Farley,[52] S. Farry,[59] D. Fazzini,[11] P. Fedin,[38] M. Féo,[47] P. Fernandez Declara,[47] A. Fernandez Prieto,[45] F. Ferrari,[19,c] L. Ferreira Lopes,[48] F. Ferreira Rodrigues,[2] S. Ferreres Sole,[31] M. Ferrillo,[49] M. Ferro-Luzzi,[47] S. Filippov,[40] R. A. Fini,[18] M. Fiorini,[20,f] M. Firlej,[34] K. M. Fischer,[62] C. Fitzpatrick,[47] T. Fiutowski,[34] F. Fleuret,[11,a] M. Fontana,[47] F. Fontanelli,[23,b] R. Forty,[47] V. Franco Lima,[59] M. Franco Sevilla,[65] M. Frank,[47] C. Frei,[47] D. A. Friday,[58] J. Fu,[25,m] W. Fuehring,[14] W. Funk,[47] E. Gabriel,[57] A. Gallas Torreira,[45] D. Galli,[19,c] S. Gallorini,[27] S. Gambetta,[57] Y. Gan,[3] M. Gandelman,[2] P. Gandini,[25] Y. Gao,[4] L. M. Garcia Martin,[46] J. García Pardiñas,[49] B. Garcia Plana,[45] F. A. Garcia Rosales,[11] J. Garra Tico,[54] L. Garrido,[44] D. Gascon,[44] C. Gaspar,[47] D. Gerick,[16] E. Gersabeck,[61] M. Gersabeck,[61] T. Gershon,[55] D. Gerstel,[10] Ph. Ghez,[8] V. Gibson,[54] A. Gioventù,[45] O. G. Girard,[48] P. Gironella Gironell,[44] L. Giubega,[36] C. Giugliano,[20] K. Gizdov,[57] V. V. Gligorov,[12] C. Göbel,[70] D. Golubkov,[38] A. Golutvin,[60,77] A. Gomes,[1,n] P. Gorbounov,[38,6] I. V. Gorelov,[39] C. Gotti,[24,g] E. Govorkova,[31] J. P. Grabowski,[16] R. Graciani Diaz,[44] T. Grammatico,[12] L. A. Granado Cardoso,[47] E. Graugés,[44] E. Graverini,[48] G. Graziani,[21] A. Grecu,[36] R. Greim,[31] P. Griffith,[20] L. Grillo,[61] L. Gruber,[47] B. R. Gruberg Cazon,[62] C. Gu,[3] E. Gushchin,[40] A. Guth,[13] Yu. Guz,[43,47] T. Gys,[47] P. Günther,[16] T. Hadavizadeh,[62] G. Haefeli,[48] C. Haen,[47] S. C. Haines,[54] P. M. Hamilton,[65] Q. Han,[7] X. Han,[16] T. H. Hancock,[62] S. Hansmann-Menzemer,[16] N. Harnew,[62] T. Harrison,[59] R. Hart,[31] C. Hasse,[47] M. Hatch,[47] J. He,[5] M. Hecker,[60] K. Heijhoff,[31] K. Heinicke,[14] A. Heister,[14] A. M. Hennequin,[47] K. Hennessy,[59] L. Henry,[46] J. Heuel,[13] A. Hicheur,[68] D. Hill,[62] M. Hilton,[61] P. H. Hopchev,[48] J. Hu,[16] W. Hu,[7] W. Huang,[5] W. Hulsbergen,[31] T. Humair,[60] R. J. Hunter,[55] M. Hushchyn,[78] D. Hutchcroft,[59] D. Hynds,[31] P. Ibis,[14] M. Idzik,[34] P. Ilten,[52] A. Inglessi,[37] A. Inyakin,[43] K. Ivshin,[37] R. Jacobsson,[47] S. Jakobsen,[47] E. Jans,[31] B. K. Jashal,[46] A. Jawahery,[65] V. Jevtic,[14] F. Jiang,[3] M. John,[62] D. Johnson,[47] C. R. Jones,[54] B. Jost,[47] N. Jurik,[62] S. Kandybei,[50] M. Karacson,[47] J. M. Kariuki,[53] N. Kazeev,[78] M. Kecke,[16] F. Keizer,[54,54] M. Kelsey,[67] M. Kenzie,[55] T. Ketel,[32] B. Khanji,[47] A. Kharisova,[79] K. E. Kim,[67] T. Kirn,[13] V. S. Kirsebom,[48] S. Klaver,[22] K. Klimaszewski,[35] S. Koliiev,[51] A. Kondybayeva,[77] A. Konoplyannikov,[38] P. Kopciewicz,[34] R. Kopecna,[16] P. Koppenburg,[31] I. Kostiuk,[31,51] O. Kot,[51] S. Kotriakhova,[37] L. Kravchuk,[40] R. D. Krawczyk,[47] M. Kreps,[55] F. Kress,[60] S. Kretzschmar,[13] P. Krokovny,[42,e] W. Krupa,[34] W. Krzemien,[35] W. Kucewicz,[33,o] M. Kucharczyk,[33] V. Kudryavtsev,[42,e] H. S. Kuindersma,[31] G. J. Kunde,[66] T. Kvaratskheliya,[38] D. Lacarrere,[47] G. Lafferty,[61] A. Lai,[26] D. Lancierini,[49] J. J. Lane,[61] G. Lanfranchi,[22] C. Langenbruch,[13] O. Lantwin,[49] T. Latham,[55] F. Lazzari,[28,p] C. Lazzeroni,[52] R. Le Gac,[10] R. Lefèvre,[9] A. Leflat,[39] O. Leroy,[10] T. Lesiak,[33] B. Leverington,[16] H. Li,[71] X. Li,[66] Y. Li,[6] Z. Li,[67] X. Liang,[67] R. Lindner,[47] V. Lisovskyi,[14] G. Liu,[71] X. Liu,[3] D. Loh,[55] A. Loi,[26] J. Lomba Castro,[45] I. Longstaff,[58] J. H. Lopes,[2] G. Loustau,[49] G. H. Lovell,[54] Y. Lu,[6] D. Lucchesi,[27,q] M. Lucio Martinez,[31] Y. Luo,[3] A. Lupato,[27] E. Luppi,[20,f] O. Lupton,[55] A. Lusiani,[28,r] X. Lyu,[5] S. Maccolini,[19,c] F. Machefert,[11] F. Maciuc,[36] V. Macko,[48] P. Mackowiak,[14] S. Maddrell-Mander,[53] L. R. Madhan Mohan,[53] O. Maev,[37,47] A. Maevskiy,[78] D. Maisuzenko,[37] M. W. Majewski,[34] S. Malde,[62] B. Malecki,[47] A. Malinin,[76] T. Maltsev,[42,e] H. Malygina,[16] G. Manca,[26,s] G. Mancinelli,[10] R. Manera Escalero,[44] D. Manuzzi,[19,c] D. Marangotto,[25,m] J. Maratas,[9,t] J. F. Marchand,[8] U. Marconi,[19] S. Mariani,[21] C. Marin Benito,[11] M. Marinangeli,[48] P. Marino,[48] J. Marks,[16] P. J. Marshall,[59] G. Martellotti,[30] L. Martinazzoli,[47] M. Martinelli,[24,g] D. Martinez Santos,[45] F. Martinez Vidal,[46] A. Massafferri,[1] M. Materok,[13] R. Matev,[47] A. Mathad,[49] Z. Mathe,[47] V. Matiunin,[38] C. Matteuzzi,[24] K. R. Mattioli,[80] A. Mauri,[49] E. Maurice,[11,a] M. McCann,[60] L. Mcconnell,[17] A. McNab,[61] R. McNulty,[17] J. V. Mead,[59] B. Meadows,[64] C. Meaux,[10] G. Meier,[14] N. Meinert,[74] D. Melnychuk,[35] S. Meloni,[24,g] M. Merk,[31] A. Merli,[25] M. Mikhasenko,[47] D. A. Milanes,[73] E. Millard,[55] M.-N. Minard,[8] O. Mineev,[38] L. Minzoni,[20,f] S. E. Mitchell,[57] B. Mitreska,[61] D. S. Mitzel,[47] A. Mödden,[14] A. Mogini,[12] R. D. Moise,[60] T. Mombächer,[14] I. A. Monroy,[73] S. Monteil,[9]

M. Morandin,[27] G. Morello,[22] M. J. Morello,[28,r] J. Moron,[34] A. B. Morris,[10] A. G. Morris,[55] R. Mountain,[67] H. Mu,[3] F. Muheim,[57] M. Mukherjee,[7] M. Mulder,[31] D. Müller,[47] K. Müller,[49] V. Müller,[14] C. H. Murphy,[62] D. Murray,[61] P. Muzzetto,[26] P. Naik,[53] T. Nakada,[48] R. Nandakumar,[56] A. Nandi,[62] T. Nanut,[48] I. Nasteva,[2] M. Needham,[57] N. Neri,[25,m] S. Neubert,[16] N. Neufeld,[47] R. Newcombe,[60] T. D. Nguyen,[48] C. Nguyen-Mau,[48,u] E. M. Niel,[11] S. Nieswand,[13] N. Nikitin,[39] N. S. Nolte,[47] C. Nunez,[80] A. Oblakowska-Mucha,[34] V. Obraztsov,[43] S. Ogilvy,[58] D. P. O'Hanlon,[19] R. Oldeman,[26,s] C. J. G. Onderwater,[75] J. D. Osborn,[80] A. Ossowska,[33] J. M. Otalora Goicochea,[2] T. Ovsiannikova,[38] P. Owen,[49] A. Oyanguren,[46] P. R. Pais,[48] T. Pajero,[28,r] A. Palano,[18] M. Palutan,[22] G. Panshin,[79] A. Papanestis,[56] M. Pappagallo,[57] L. L. Pappalardo,[20,f] C. Pappenheimer,[64] W. Parker,[65] C. Parkes,[61] G. Passaleva,[21,47] A. Pastore,[18] M. Patel,[60] C. Patrignani,[19,c] A. Pearce,[47] A. Pellegrino,[31] M. Pepe Altarelli,[47] S. Perazzini,[19] D. Pereima,[38] P. Perret,[9] L. Pescatore,[48] K. Petridis,[53] A. Petrolini,[23,b] A. Petrov,[76] S. Petrucci,[57] M. Petruzzo,[25,m] B. Pietrzyk,[8] G. Pietrzyk,[48] M. Pili,[62] D. Pinci,[30] J. Pinzino,[47] F. Pisani,[47] A. Piucci,[16] V. Placinta,[36] S. Playfer,[57] J. Plews,[52] M. Plo Casasus,[45] F. Polci,[12] M. Poli Lener,[22] M. Poliakova,[67] A. Poluektov,[10] N. Polukhina,[77,v] I. Polyakov,[67] E. Polycarpo,[2] G. J. Pomery,[53] S. Ponce,[47] A. Popov,[43] D. Popov,[52] S. Poslavskii,[43] K. Prasanth,[33] L. Promberger,[47] C. Prouve,[45] V. Pugatch,[51] A. Puig Navarro,[49] H. Pullen,[62] G. Punzi,[28,i] W. Qian,[5] J. Qin,[5] R. Quagliani,[12] B. Quintana,[9] N. V. Raab,[17] R. I. Rabadan Trejo,[10] B. Rachwal,[34] J. H. Rademacker,[53] M. Rama,[28] M. Ramos Pernas,[45] M. S. Rangel,[2] F. Ratnikov,[41,78] G. Raven,[32] M. Reboud,[8] F. Redi,[48] F. Reiss,[12] C. Remon Alepuz,[46] Z. Ren,[3] V. Renaudin,[62] S. Ricciardi,[56] S. Richards,[53] K. Rinnert,[59] P. Robbe,[11] A. Robert,[12] A. B. Rodrigues,[48] E. Rodrigues,[64] J. A. Rodriguez Lopez,[73] M. Roehrken,[47] S. Roiser,[47] A. Rollings,[62] V. Romanovskiy,[43] M. Romero Lamas,[45] A. Romero Vidal,[45] J. D. Roth,[80] M. Rotondo,[22] M. S. Rudolph,[67] T. Ruf,[47] J. Ruiz Vidal,[46] J. Ryzka,[34] J. J. Saborido Silva,[45] N. Sagidova,[37] B. Saitta,[26,s] C. Sanchez Gras,[31] C. Sanchez Mayordomo,[46] R. Santacesaria,[30] C. Santamarina Rios,[45] M. Santimaria,[22] E. Santovetti,[29,w] G. Sarpis,[61] A. Sarti,[30] C. Satriano,[30,x] A. Satta,[29] M. Saur,[5] D. Savrina,[38,39] L. G. Scantlebury Smead,[62] S. Schael,[13] M. Schellenberg,[14] M. Schiller,[58] H. Schindler,[47] M. Schmelling,[15] T. Schmelzer,[14] B. Schmidt,[47] O. Schneider,[48] A. Schopper,[47] H. F. Schreiner,[64] M. Schubiger,[31] S. Schulte,[48] M. H. Schune,[11] R. Schwemmer,[47] B. Sciascia,[22] A. Sciubba,[30,y] S. Sellam,[68] A. Semennikov,[38] A. Sergi,[52,47] N. Serra,[49] J. Serrano,[10] L. Sestini,[27] A. Seuthe,[14] P. Seyfert,[47] D. M. Shangase,[80] M. Shapkin,[43] L. Shchutska,[48] T. Shears,[59] L. Shekhtman,[42,e] V. Shevchenko,[76,77] E. Shmanin,[77] J. D. Shupperd,[67] B. G. Siddi,[20] R. Silva Coutinho,[49] L. Silva de Oliveira,[2] G. Simi,[27,q] S. Simone,[18,k] I. Skiba,[20] N. Skidmore,[16] T. Skwarnicki,[67] M. W. Slater,[52] J. G. Smeaton,[54] A. Smetkina,[38] E. Smith,[13] I. T. Smith,[57] M. Smith,[60] A. Snoch,[31] M. Soares,[19] L. Soares Lavra,[1] M. D. Sokoloff,[64] F. J. P. Soler,[58] B. Souza De Paula,[2] B. Spaan,[14] E. Spadaro Norella,[25,m] P. Spradlin,[58] F. Stagni,[47] M. Stahl,[64] S. Stahl,[47] P. Stefko,[48] O. Steinkamp,[49] S. Stemmle,[16] O. Stenyakin,[43] M. Stepanova,[37] H. Stevens,[14] S. Stone,[67] S. Stracka,[28] M. E. Stramaglia,[48] M. Straticiuc,[36] S. Strokov,[79] J. Sun,[3] L. Sun,[72] Y. Sun,[65] P. Svihra,[61] K. Swientek,[34] A. Szabelski,[35] T. Szumlak,[34] M. Szymanski,[5] S. Taneja,[61] Z. Tang,[3] T. Tekampe,[14] G. Tellarini,[20] F. Teubert,[47] E. Thomas,[47] K. A. Thomson,[59] M. J. Tilley,[60] V. Tisserand,[9] S. T'Jampens,[8] M. Tobin,[6] S. Tolk,[47] L. Tomassetti,[20,f] D. Tonelli,[28] D. Torres Machado,[1] D. Y. Tou,[12] E. Tournefier,[8] M. Traill,[58] M. T. Tran,[48] C. Trippl,[48] A. Trisovic,[54] A. Tsaregorodtsev,[10] G. Tuci,[28,47,i] A. Tully,[48] N. Tuning,[31] A. Ukleja,[35] A. Usachov,[11] A. Ustyuzhanin,[41,78] U. Uwer,[16] A. Vagner,[79] V. Vagnoni,[19] A. Valassi,[47] G. Valenti,[19] M. van Beuzekom,[31] H. Van Hecke,[66] E. van Herwijnen,[47] C. B. Van Hulse,[17] M. van Veghel,[75] R. Vazquez Gomez,[44] P. Vazquez Regueiro,[45] C. Vázquez Sierra,[31] S. Vecchi,[20] J. J. Velthuis,[53] M. Veltri,[21,z] A. Venkateswaran,[67] M. Vernet,[9] M. Veronesi,[31] M. Vesterinen,[55] J. V. Viana Barbosa,[47] D. Vieira,[5] M. Vieites Diaz,[48] H. Viemann,[74] X. Vilasis-Cardona,[44,h] A. Vitkovskiy,[31] V. Volkov,[39] A. Vollhardt,[49] D. Vom Bruch,[12] A. Vorobyev,[37] V. Vorobyev,[42,e] N. Voropaev,[37] R. Waldi,[74] J. Walsh,[28] J. Wang,[3] J. Wang,[72] J. Wang,[6] M. Wang,[3] Y. Wang,[7] Z. Wang,[49] D. R. Ward,[54] H. M. Wark,[59] N. K. Watson,[52] D. Websdale,[60] A. Weiden,[49] C. Weisser,[63] B. D. C. Westhenry,[53] D. J. White,[61] M. Whitehead,[13] D. Wiedner,[14] G. Wilkinson,[62] M. Wilkinson,[67] I. Williams,[54] M. Williams,[63] M. R. J. Williams,[61] T. Williams,[52] F. F. Wilson,[56] W. Wislicki,[35] M. Witek,[33] L. Witola,[16] G. Wormser,[11] S. A. Wotton,[54] H. Wu,[67] K. Wyllie,[47] Z. Xiang,[5] D. Xiao,[7] Y. Xie,[7] H. Xing,[71] A. Xu,[3] L. Xu,[3] M. Xu,[7] Q. Xu,[5] Z. Xu,[8] Z. Xu,[4] Z. Yang,[3] Z. Yang,[65] Y. Yao,[67] L. E. Yeomans,[59] H. Yin,[7] J. Yu,[7,aa] X. Yuan,[67] O. Yushchenko,[43] K. A. Zarebski,[52] M. Zavertyaev,[15,v] M. Zdybal,[33] M. Zeng,[3] D. Zhang,[7] L. Zhang,[3] S. Zhang,[3] W. C. Zhang,[3,bb] Y. Zhang,[47] A. Zhelezov,[16] Y. Zheng,[5] X. Zhou,[5] Y. Zhou,[5] X. Zhu,[3] V. Zhukov,[13,39] J. B. Zonneveld,[57] and S. Zucchelli[19,c]

(LHCb Collaboration)

[1]*Centro Brasiliero de Pesquisas Físicas (CBPF), Rio de Janeiro, Brazil*

[2]*Universidade Federal do Rio de Janeiro (UFRJ), Rio de Janeiro, Brazil*

[3]*Center for High Energy Physics, Tsinghua University, Beijing, China*

[4]*School of Physics State Key Laboratory of Nuclear Physics and Technology, Peking University, Beijing, China*

[5]*University of Chinese Academy of Sciences, Beijing, China*

[6]*Institute Of High Energy Physics (IHEP), Beijing, China*

[7]*Institute of Particle Physics, Central China Normal University, Wuhan, Hubei, China*

[8]*Univ. Grenoble Alpes, Univ. Savoie Mont Blanc, CNRS, IN2P3-LAPP, Annecy, France*

[9]*Université Clermont Auvergne, CNRS/IN2P3, LPC, Clermont-Ferrand, France*

[10]*Aix Marseille Univ, CNRS/IN2P3, CPPM, Marseille, France*

[11]*LAL, Univ. Paris-Sud, CNRS/IN2P3, Université Paris-Saclay, Orsay, France*

[12]*LPNHE, Sorbonne Université, Paris Diderot Sorbonne Paris Cité, CNRS/IN2P3, Paris, France*

[13]*I. Physikalisches Institut, RWTH Aachen University, Aachen, Germany*

[14]*Fakultät Physik, Technische Universität Dortmund, Dortmund, Germany*

[15]*Max-Planck-Institut für Kernphysik (MPIK), Heidelberg, Germany*

[16]*Physikalisches Institut, Ruprecht-Karls-Universität Heidelberg, Heidelberg, Germany*

[17]*School of Physics, University College Dublin, Dublin, Ireland*

[18]*INFN Sezione di Bari, Bari, Italy*

[19]*INFN Sezione di Bologna, Bologna, Italy*

[20]*INFN Sezione di Ferrara, Ferrara, Italy*

[21]*INFN Sezione di Firenze, Firenze, Italy*

[22]*INFN Laboratori Nazionali di Frascati, Frascati, Italy*

[23]*INFN Sezione di Genova, Genova, Italy*

[24]*INFN Sezione di Milano-Bicocca, Milano, Italy*

[25]*INFN Sezione di Milano, Milano, Italy*

[26]*INFN Sezione di Cagliari, Monserrato, Italy*

[27]*INFN Sezione di Padova, Padova, Italy*

[28]*INFN Sezione di Pisa, Pisa, Italy*

[29]*INFN Sezione di Roma Tor Vergata, Roma, Italy*

[30]*INFN Sezione di Roma La Sapienza, Roma, Italy*

[31]*Nikhef National Institute for Subatomic Physics, Amsterdam, Netherlands*

[32]*Nikhef National Institute for Subatomic Physics and VU University Amsterdam, Amsterdam, Netherlands*

[33]*Henryk Niewodniczanski Institute of Nuclear Physics Polish Academy of Sciences, Kraków, Poland*

[34]*AGH—University of Science and Technology, Faculty of Physics and Applied Computer Science, Kraków, Poland*

[35]*National Center for Nuclear Research (NCBJ), Warsaw, Poland*

[36]*Horia Hulubei National Institute of Physics and Nuclear Engineering, Bucharest-Magurele, Romania*

[37]*Petersburg Nuclear Physics Institute NRC Kurchatov Institute (PNPI NRC KI), Gatchina, Russia*

[38]*Institute of Theoretical and Experimental Physics NRC Kurchatov Institute (ITEP NRC KI), Moscow, Russia, Moscow, Russia*

[39]*Institute of Nuclear Physics, Moscow State University (SINP MSU), Moscow, Russia*

[40]*Institute for Nuclear Research of the Russian Academy of Sciences (INR RAS), Moscow, Russia*

[41]*Yandex School of Data Analysis, Moscow, Russia*

[42]*Budker Institute of Nuclear Physics (SB RAS), Novosibirsk, Russia*

[43]*Institute for High Energy Physics NRC Kurchatov Institute (IHEP NRC KI), Protvino, Russia, Protvino, Russia*

[44]*ICCUB, Universitat de Barcelona, Barcelona, Spain*

[45]*Instituto Galego de Física de Altas Enerxías (IGFAE), Universidade de Santiago de Compostela, Santiago de Compostela, Spain*

[46]*Instituto de Fisica Corpuscular, Centro Mixto Universidad de Valencia—CSIC, Valencia, Spain*

[47]*European Organization for Nuclear Research (CERN), Geneva, Switzerland*

[48]*Institute of Physics, Ecole Polytechnique Fédérale de Lausanne (EPFL), Lausanne, Switzerland*

[49]*Physik-Institut, Universität Zürich, Zürich, Switzerland*

[50]*NSC Kharkiv Institute of Physics and Technology (NSC KIPT), Kharkiv, Ukraine*

[51]*Institute for Nuclear Research of the National Academy of Sciences (KINR), Kyiv, Ukraine*

[52]*University of Birmingham, Birmingham, United Kingdom*

[53]*H.H. Wills Physics Laboratory, University of Bristol, Bristol, United Kingdom*

[54]*Cavendish Laboratory, University of Cambridge, Cambridge, United Kingdom*

[55]*Department of Physics, University of Warwick, Coventry, United Kingdom*

[56]*STFC Rutherford Appleton Laboratory, Didcot, United Kingdom*

[57]*School of Physics and Astronomy, University of Edinburgh, Edinburgh, United Kingdom*

[58]*School of Physics and Astronomy, University of Glasgow, Glasgow, United Kingdom*

[59]*Oliver Lodge Laboratory, University of Liverpool, Liverpool, United Kingdom*

[60]Imperial College London, London, United Kingdom

[61]Department of Physics and Astronomy, University of Manchester, Manchester, United Kingdom

[62]Department of Physics, University of Oxford, Oxford, United Kingdom

[63]Massachusetts Institute of Technology, Cambridge, Massachusetts, USA

[64]University of Cincinnati, Cincinnati, Ohio, USA

[65]University of Maryland, College Park, Maryland, USA

[66]Los Alamos National Laboratory (LANL), Los Alamos, USA

[67]Syracuse University, Syracuse, New York, USA

[68]Laboratory of Mathematical and Subatomic Physics, Constantine, Algeria

[associated with Universidade Federal do Rio de Janeiro (UFRJ), Rio de Janeiro, Brazil]

[69]School of Physics and Astronomy, Monash University, Melbourne, Australia

(associated with Department of Physics, University of Warwick, Coventry, United Kingdom)

[70]Pontifícia Universidade Católica do Rio de Janeiro (PUC-Rio), Rio de Janeiro, Brazil

[associated with Universidade Federal do Rio de Janeiro (UFRJ), Rio de Janeiro, Brazil]

[71]South China Normal University, Guangzhou, China

(associated with Center for High Energy Physics, Tsinghua University, Beijing, China)

[72]School of Physics and Technology, Wuhan University, Wuhan, China

(associated with Center for High Energy Physics, Tsinghua University, Beijing, China)

[73]Departamento de Fisica, Universidad Nacional de Colombia, Bogota, Colombia

(associated with LPNHE, Sorbonne Université, Paris Diderot Sorbonne Paris Cité, CNRS/IN2P3, Paris, France)

[74]Institut für Physik, Universität Rostock, Rostock, Germany

(associated with Physikalisches Institut, Ruprecht-Karls-Universität Heidelberg, Heidelberg, Germany)

[75]Van Swinderen Institute, University of Groningen, Groningen, Netherlands

(associated with Nikhef National Institute for Subatomic Physics, Amsterdam, Netherlands)

[76]National Research Centre Kurchatov Institute, Moscow, Russia

[associated with Institute of Theoretical and Experimental Physics NRC Kurchatov Institute (ITEP NRC KI),

Moscow, Russia, Moscow, Russia]

[77]National University of Science and Technology "MISIS", Moscow, Russia

[associated with Institute of Theoretical and Experimental Physics NRC Kurchatov Institute (ITEP NRC KI),

Moscow, Russia, Moscow, Russia]

[78]National Research University Higher School of Economics, Moscow, Russia

(associated with Yandex School of Data Analysis, Moscow, Russia)

[79]National Research Tomsk Polytechnic University, Tomsk, Russia

[associated with Institute of Theoretical and Experimental Physics NRC Kurchatov Institute (ITEP NRC KI),

Moscow, Russia, Moscow, Russia]

[80]University of Michigan, Ann Arbor, USA

[associated with Syracuse University, Syracuse, New York, USA]

[a]Also at Laboratoire Leprince-Ringuet, Palaiseau, France.

[b]Also at Università di Genova, Genova, Italy.

[c]Also at Università di Bologna, Bologna, Italy.

[d]Also at Università di Modena e Reggio Emilia, Modena, Italy.

[e]Also at Novosibirsk State University, Novosibirsk, Russia.

[f]Also at Università di Ferrara, Ferrara, Italy.

[g]Also at Università di Milano Bicocca, Milano, Italy.

[h]Also at DS4DS, La Salle, Universitat Ramon Llull, Barcelona, Spain.

[i]Also at Università di Pisa, Pisa, Italy.

[j]Also at Universidad Nacional Autonoma de Honduras, Tegucigalpa, Honduras.

[k]Also at Università di Bari, Bari, Italy.

[l]Also at INFN Sezione di Trieste, Trieste, Italy.

[m]Also at Università degli Studi di Milano, Milano, Italy.

[n]Also at Universidade Federal do Triângulo Mineiro (UFTM), Uberaba-MG, Brazil.

[o]Also at AGH—University of Science and Technology, Faculty of Computer Science, Electronics and Telecommunications, Kraków, Poland.

[p]Also at Università di Siena, Siena, Italy.

[q]Also at Università di Padova, Padova, Italy.

[r]Also at Scuola Normale Superiore, Pisa, Italy.

[s]Also at Università di Cagliari, Cagliari, Italy.

[t]Also at MSU—Iligan Institute of Technology (MSU-IIT), Iligan, Philippines.

[u]Also at Hanoi University of Science, Hanoi, Vietnam.

[v]Also at P.N. Lebedev Physical Institute, Russian Academy of Science (LPI RAS), Moscow, Russia.

[w]Also at Università di Roma Tor Vergata, Roma, Italy.

[x]Also at Università della Basilicata, Potenza, Italy.

[y]Also at Università di Roma La Sapienza, Roma, Italy.

[z]Also at Università di Urbino, Urbino, Italy.

[aa]Also at Physics and Micro Electronic College, Hunan University, Changsha City, China.

[bb]Also at School of Physics and Information Technology, Shaanxi Normal University (SNNU), Xi'an, China.